Molecular effects in solid $NaNO_3$ observed by x-ray absorption and resonant Auger spectroscopy

A. B. Preobrajenski,[1,2,*] A. S. Vinogradov,[1] S. L. Molodtsov,[3] S. K. Krasnikov,[1,2] T. Chassé,[2,4] R. Szargan,[2] and C. Laubschat[3]

[1]*Institute of Physics, St. Petersburg State University, 198504 St. Petersburg, Russia*

[2]*Wilhelm-Ostwald-Institut für Physikalische und Theoretische Chemie, Universität Leipzig, D-04103 Leipzig, Germany*

[3]*Institut für Oberflächen- und Mikrostrukturphysik, Technische Universität Dresden, D-01062 Dresden, Germany*

[4]*Institut für Oberflächenmodifizierung, D-04318 Leipzig, Germany*

(Received 19 December 2001; published 15 May 2002)

X-ray absorption and resonant Auger spectroscopy were used to study the formation and decay of nitrogen and oxygen core excitations in ionic-molecular solid $NaNO_3$. It has been shown that the most prominent features in the electronic structure of both valence and conduction bands of the $NaNO_3$ crystal are determined by molecular states of the quasi-isolated NO_3^- group. In the Auger decay following the strongly localized N $1s \rightarrow 2a_2''(\pi)$ and O $1s \rightarrow 2a_2''(\pi)$ core excitations both spectator and participator signals of extremely high intensity have been found. The nuclear out-of-plane motion inside the NO_3^- group has been shown to be observable by resonant Auger spectroscopy as a strongly non-Raman dispersion of individual participator features upon tuning the photon energy across the N $1s \rightarrow 2a_2''(\pi)$ and O $1s \rightarrow 2a_2''(\pi)$ resonances. All results on electronic and vibrational properties of $NaNO_3$ are compared with those of the gas-phase BF_3 molecule, which is isoelectronic and isostructural to the NO_3^- group.

DOI: 10.1103/PhysRevB.65.205116 PACS number(s): 78.70.Dm, 32.80.Hd, 33.20.Rm, 79.60.−i

I. INTRODUCTION

Due to the advent of high-brilliance synchrotron radiation sources, the combination of x-ray absorption and resonant Auger spectroscopy represents nowadays a very efficient tool for studying electronic structure and post-collision behavior of atoms, molecules, and solids. In particular, a wealth of phenomena in formation and decay of the core-excited states has been found and explained for the strongly correlated materials like lanthanides, actinides, and $3d$ transition-metal compounds,[1] as well as for simple molecules with the first-row atoms[2,3] and adsorbates.[4] In spite of the apparent structural dissimilarity between simple molecules and solids with strong electron correlation, these objects possess one common property, which determines a considerable promise of resonant methods for studying electronic nature of such systems, namely, the high degree of localization of their intermediate core-excited states. Moreover, for the resonant behavior of a core-excited system a strong coupling between the valence electrons and electrons promoted into initially unoccupied localized orbitals is necessary. The best coupling can be achieved if the valence states and the low-lying unfilled orbitals are of the same nature, as is typical for simple molecules with light elements ($2p$-state coupling), transition-metal compounds ($3d$-state coupling), or lanthanides ($4f$-state coupling). On the other hand, a strong localization of core excitations combined with the similar origin of upper filled and lower unfilled orbitals is characteristic not only for these systems. In principle, one can expect localized behavior of this kind in every solid containing quasi-isolated molecularlike groups of light elements (CO, NO^-, CN^-, NO_2^-, etc.) as structural units. Such compounds are numerous and their investigation by resonant methods involving core excitations is very promising. In particular, a lot can be learned about the origin of core excitations and their relation to electronic structure as well as their decay processes in these solids by comparing resonant spectra of their quasimolecular anions with those of isoelectronic and isostructural free molecules. Surprisingly, such studies are still rare.

The ionic-molecular crystals MNO_2 and MNO_3 ($M=$ Li, Na, K) with the planar anions NO_2^- and NO_3^-, respectively, represent a prototypical example of the solids with quasi-isolated polyatomic units. The chemical bonding inside NO_2^- and NO_3^- is essentially covalent, whereas the cation-anion interaction is rather ionic. Recently we have reported on the first combined x-ray absorption and resonant photoemission study of $NaNO_2$ at the O $1s$ and N $1s$ edges,[5] which has demonstrated the effect of the coexistence and huge intensities of the spectator and participator decay channels upon the excitation of oxygen and nitrogen core electrons into the lowest unoccupied state of the crystal. This result was interpreted in terms of strong localization of this intermediate state on the NO_2^- group due to its essentially quasimolecular nature.

In this article we report on the formation and decay of core excitations in another ionic-molecular solid $NaNO_3$. Sodium nitrate is a wide-band-gap ionic material with the rhombohedral lattice of calcite (space group D_{3d}^6 at room temperature) and lattice constants $a=b=5.071$ Å and $c=16.825$ Å.[6] The symmetry of the isolated NO_3^- anion is D_{3h}, and the site symmetry of NO_3^- in the distorted octahedral surrounding of six neighboring Na^+ ions is D_{3d}. The NO_3^- group is isoelectronic and isostructural to the free molecule BF_3. This fact manifests itself in the observed similarity in x-ray absorption near-edge structure (XANES) between the B $1s$ absorption spectrum of BF_3 and the N $1s$ one of $NaNO_3$, as discussed in Refs. 7 and 8. Recently resonance Auger spectra of BF_3 in vicinity of the strong π-resonance B $1s \rightarrow 2a_2''$ were obtained and interpreted in terms of competition between the decay of core-excited electronic states and

the fragmentation processes.[9–14] It has been shown that the core-excited molecule deforms to the pyramidal C_{3v} structure due to the movement of the B atom out of the molecular plane[11,13] prior to the molecule dissociation with the ejection of energetic B^+ ions in the same out-of-plane direction.[10] On the other hand, the NO_3^- anion in $NaNO_3$ can be approximately thought of as a ''BF_3 molecule'' placed into a ''cage'' of Na^+ ions. This ionic surrounding should suppress the fragmentation of the molecule (anion) but not its internal vibration, providing the possibility to concentrate on the study of decay processes in a movable but only weakly dissociating system. Since high-resolution resonant Auger spectroscopy has been found very sensitive to the nuclear motion in case of BF_3, it is of high interest to apply it to $NaNO_3$ in attempt to reveal any signatures of nuclear dynamics also in case of a solid.

Thus, the main goal of the present work is to investigate the role of electronic and vibrational properties of the NO_3^- anion in the formation and decay processes of nitrogen and oxygen core excitations in solid $NaNO_3$.

II. EXPERIMENT

The experiments were performed at the D1011 beamline at MAX II storage ring in Lund, Sweden. The beamline is equipped with a modified SX-700 plane grating monochromator and a high-resolution SES-200 electron energy analyzer at the end station. The photon energy resolution was set to 200 meV at the N *K* edge and to 300 meV at the O *K* edge, and the kinetic energy resolution to 150 meV. An MCP detector was used for the absorption measurements in the total electron yield mode. The basis pressure during the measurements was in the range of $1-2\times10^{-10}$ mbar. Additionally, highly resolved core-level and valence-band x-ray photoemission spectra (XPS) spectra of $NaNO_3$ were measured with monochromatized Al $K\alpha$ radiation using an Escalab 220iXL spectrometer at the Wilhelm-Ostwald-Institute for Physical and Theoretical Chemistry in Leipzig.

The samples were thin (20-30 nm) polycrystalline $NaNO_3$ films deposited *in situ* with a molecular beam from a single water-cooled effusion cell of Knudsen type onto a clean polished copper plate in a vacuum of 5×10^{-8} mbar. This preparation allows us to obtain samples free of contaminants and to avoid charging effects. The cell was filled with highly purified sodium nitrate (provided by Alfa Aesar), which was thoroughly dehydrated before the evaporation for several hours. The deposition temperatures were in the range of 320–340 °C, slightly above the melting point (308 °C) but below the decomposition point (380 °C). A small amount of decomposed species (probably NO_2^- ions located at the surface of the individual crystallites) never exceeded 5% as could be judged from the absorption spectra. This species does not disturb our resonant study, since its π resonance is energetically separated from that of $NaNO_3$. The following x-ray irradiation of the samples was found to result in only minor further decomposition, so that almost no changes could be detected in the spectra after some hours of measurements. Nevertheless, the position of the light spot on the sample was varied every 2 h in order to ensure insignificance of chemical decomposition.

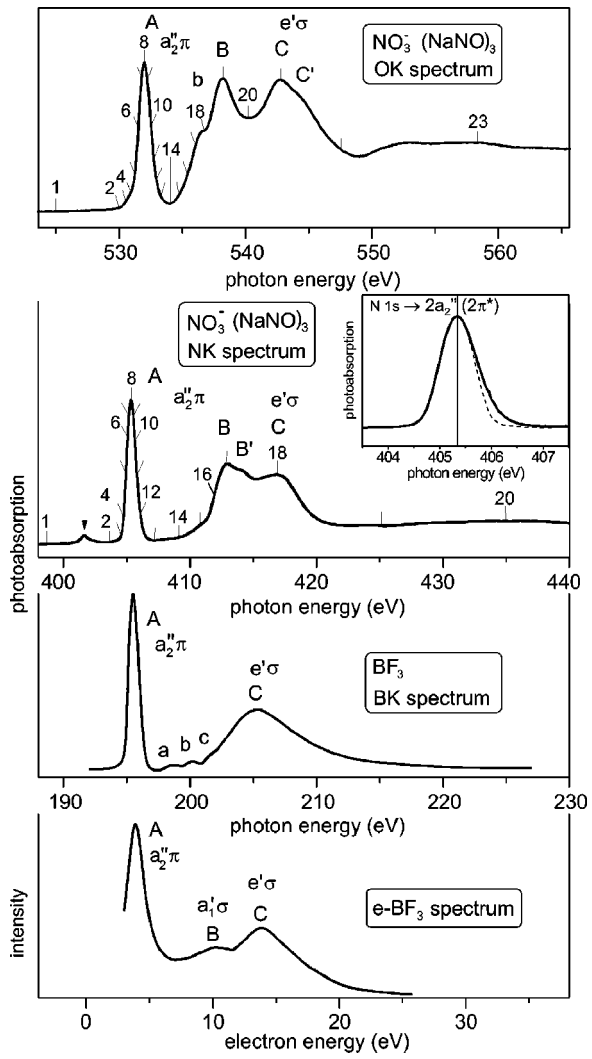

FIG. 1. O *K* and N *K* absorption spectra of solid $NaNO_3$, B *K* absorption spectrum of gas-phase BF_3 (Ref. 15) and spectrum of electron scattering on BF_3 molecules (Ref. 16). See text for energy scale alignment. Partly numbered thin strokes on O *K* and N *K* absorption curves indicate photon energies used for excitation of Auger-photoemission spectra shown in Figs. 3–6. A small black triangle at 401.5 eV on the N *K* spectrum indicates the energy position of the π resonance of the NO_2^- species resulting from slight decomposition of $NaNO_3$. Structures *a*–*c* in B 1*s* photoabsorption of BF_3 are Rydberg states of boron. Inset: enlargement of the N *K* π resonance. The dashed line (a reflected left part of the peak) is drawn to stress the peak shape asymmetry.

III. RESULTS AND DISCUSSION

A. Absorption

The photoabsorption spectra of $NaNO_3$ at the O 1*s* and N 1*s* edges are presented in Fig. 1 together with the B 1*s* absorption[15] and electron-molecular scattering[16] spectra of the gas-phase BF_3. The N 1*s*, B 1*s*, and $e-BF_3$ spectra are aligned at the position of peak *A*, while for alignment of the

N 1*s* and O 1*s* spectra the XPS-measured shift of 125.6 eV between the respective core levels is used. A weak decomposition of NO_3^- ions, which occurs during the preparation and the following irradiation, can be seen mainly as a small feature (π resonance in NO_2^-) at 401.5 eV in the N 1*s* spectrum and as a small shoulder at 531.5 eV in the O 1*s* spectrum.

The presented absorption spectra of $NaNO_3$ are better resolved than those reported earlier,[7,8,17] resulting in additional structure of band *C* in O 1*s* (*C'*) and of band *B* in N 1*s* (*B'*) as well as in the clear asymmetry of peak A in both spectra (see inset in Fig. 1 for the case of N 1*s*). Without considering fine details the general run of the absorption curves is obviously similar for the oxygen and nitrogen spectra. This is a clear indication of a strong mixing between unoccupied N 2*p* and O 2*p* orbitals, resulting in the reproduction of a common sequence of the unoccupied electronic states of $NaNO_3$ in both absorption spectra. The main features in each spectrum are the narrow band *A* below the ionization threshold and two broader bands *B* and *C* above it. As seen in Fig. 1, first of all the N 1*s* but also the O 1*s* absorption curves definitely resemble those of B 1*s* absorption and electron-molecule scattering in the gas-phase BF_3, which is isoelectronic and isostructural to the undisturbed NO_3^- group. This fact unambiguously reveals a quasimolecular nature of the nitrogen and oxygen core excitations in solid $NaNO_3$ and allows us to discuss the spectrum of unoccupied electronic states in this crystal in terms of molecular orbitals (MO's) of the quasi-isolated NO_3^- anion. As a result, the main bands *A* and *C* may be associated with the core electron transitions to unoccupied $2a_2''(\pi)$ and $4e'(\sigma)$ MO's of the planar NO_3^- anion, respectively, composed mainly of the nitrogen-oxygen $2p_z$ and $2p_{x,y}$ states, respectively. The strong anisotropy of the molecular potential of the NO_3^- group causes a large energy splitting between $2a_2''(\pi)$ and $4e'(\sigma)$ MO's, placing the corresponding resonant features *A* and *C* into different regions of the spectrum. It should be noted that the energy separation between the positions of peak *A* in the N 1*s* and O 1*s* spectra ($\sim$1 eV) may be associated with a final-state effect due to the different manifestation of the corresponding core holes in the spectra.

The origin of band *B* is more controversial. In analogy with the peak *B* in the electron-molecular scattering spectrum of BF_3 (Fig. 1), where it may appear due to the temporary electron capture by BF_3 into the $3a_1'$ MO, it may be thought of as an analog of the $1s \rightarrow 3a_1'$ transition. This transition is dipole forbidden in the B 1*s* absorption of BF_3 but could become dipole allowed for lower symmetries. The x-ray diffraction study of Göttlicher and Knöchel[18] provides evidence for the lowering of the NO_3^- point symmetry in $NaNO_3$ from D_{3h} to C_{3v} as a result of the slight (0.1 Å) shift of three oxygen atoms. These up- and down-pyramidal distortions of the NO_3^- group are supposed to be statistically averaged over the crystal, so that the space symmetry of $NaNO_3$ ($R\bar{3}c$) does not change. Thus, the $1s \rightarrow 3a_1'$ origin of *B* remains possible. In accordance with the optical measurements[19] and band-structure calculations[20] we also suppose an admixture of the Na 3*s* states into the $3a_1'$ MO. Thus, bands *A* and *C* in the O 1*s* and N 1*s* absorption have essentially molecular origin, whereas band *B* reflects both molecular and solid-state effects.

Another molecularlike feature in the absorption spectra is the asymmetry of band *A* (Fig. 1, inset). Similar slight asymmetry of the B $1s \rightarrow 2a_2''$ resonance in BF_3 has been interpreted in terms of coupling of the B $1s^{-1}2a_2''$ core excitation with the a_2'' out-of-plane bending vibration.[12,14] We suggest that the asymmetric shape of the N (and, less pronounced, O) $1s \rightarrow 2a_2''$ resonance in solid $NaNO_3$ also originates from the unresolved a_2''-vibration progression. Isolated NO_3^- belongs to the same point group D_{3h} as BF_3 and its fundamental vibration mode ν_2 (a_2'') is infrared active at 103 meV.[21] The full width at half maximum (FWHM) of the N $1s^{-1}2a_2''$ resonance in $NaNO_3$ is 850 meV, while the photon bandwidth is about 200 meV. Since the lifetime broadening of the N $1s^{-1}\pi^*(\nu=0)$ state in simple N-containing molecules (N_2, N_2O) never exceeds 115 meV,[22] several a_2'' vibration levels can be expected at the FWHM of this resonance. The fact that the time for the maximal out-of-plane displacement of the N atom (0.25 of the full period, $\sim$10 fs) is on the same scale as a lifetime of the N $1s^{-1}2a_2''$ intermediate state is of crucial importance for the decay processes, as will be discussed below. The a_2'' vibrations are expected to be highly stimulated through the $1s \rightarrow 2a_2''$ excitation.

B. Electronic structure of the valence band

Before we proceed with the discussion of deexcitation phenomena, it is necessary to describe the valence-band electronic structure of $NaNO_3$ in the ground state. This structure was recently calculated *ab initio* in the framework of periodic Hartree-Fock theory and discussed in detail in Ref. 20. Some older theoretical studies of NO_3^- based on the MO approach are also known in the literature.[23–25] For the purpose of completeness we provide below the results of our own theoretical analysis and compare them with the measured high-resolution valence-band XPS spectrum of $NaNO_3$.

The electronic structure calculations were performed within the *ab initio* plane-wave total-energy pseudopotential method[26] based on the density functional theory[27] as implemented in the code CASTEP.[28] Both local-density approximation (LDA) with the parametrization of Perdew and Zunger[29] and generalized gradient approximation (GGA) with the parametrization of Perdew and Wang[30] were tried for the description of electron exchange and correlation. The electron-ion interaction was described by ultrasoft pseudopotentials,[31] and the Na 2*s* and 2*p* electrons were explicitly treated as valence electrons. The Brillouin zone was sampled within the Monkhorst-Pack algorithm[32] with the 0.1 $Å^{-1}$ distances between sampling points. The plane-wave kinetic energy cutoff of 370 eV was used.

Prior to the electronic structure calculations the geometry optimization was performed. A trigonal unit cell of the D_{3d}^6 ($R\bar{3}c$) symmetry containing 6 Na atoms, 6 N atoms, and 18 O atoms with the experimental lattice parameters specified

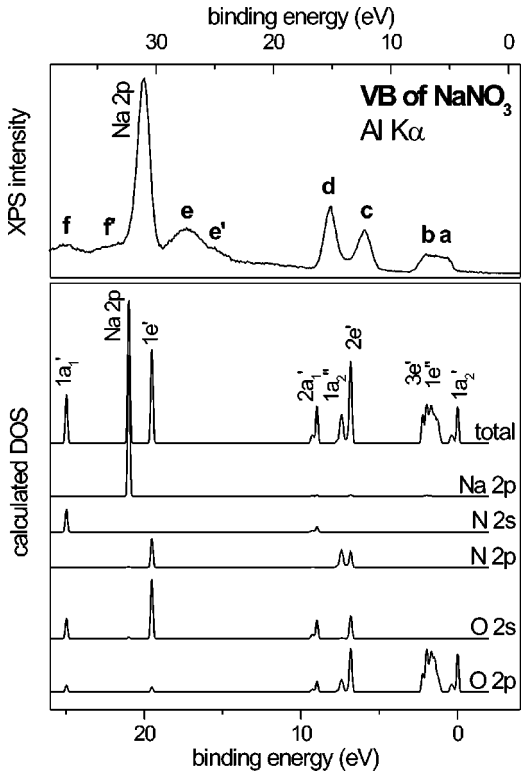

FIG. 2. Valence-band photoemission spectrum of $NaNO_3$ measured with Al $K\alpha$ (upper part) as compared with the DFT-LDA pseudopotential calculation of the total and partial ground-state DOS of $NaNO_3$ (lower part).

above has been chosen as a starting geometry. Both the LDA and GGA result in a 1%-2% deviation of the a and c lattice constants from the initial values, but the experimental ratio $a/c=0.302$ remains unchanged only for the GGA, while for the LDA it is reduced to 0.292. This is the reason why the GGA was preferred for the electronic structure calculations discussed below. It should be noted that the density of states (DOS) of the valence band obtained with the LDA differs from that obtained with the GGA only in minor details.

Figure 2 shows calculated total and partial DOS of $NaNO_3$ in comparison with the XPS spectrum of its valence band. For the theoretical curves the position of the highest occupied state is set to zero, while the binding energies of the measured spectrum refer to the Fermi level of the spectrometer. Each feature in the total DOS plot is assigned to a particular MO of the NO_3^- anion. Definitely, such an assignment does not take into account the effects of electron mixing between cation's and anion's states. Nevertheless, the MO language is quite appropriate here due to the obviously molecularlike character of the valence band and it will be used further in order to stress the genealogy of the particular features. In spite of a significant underestimation of energy separations between individual peaks in the computed DOS, the number, consecutive ordering, and relative energy positions of experimental features a-f and Na $2p$ are reproduced fairly well by the calculation (Na $2s$ is also accounted for but not shown). The only exceptions are e' and f' shoulders, which could not be reproduced also in all earlier ground-state studies and should probably be assigned to a final-state effect. The present results of the electronic structure calculations are in good agreement with the previous results for NO_3^- (Ref. 23–25) and $NaNO_3$ (Ref. 20).

The lowest-lying spectral feature a-b is associated with the MO's built up almost exclusively from the O $2p$ states: weakly bonding $3e'(\sigma)$ and nonbonding $1e''(n)$ and $1a_2'(n)$. The next band c is caused by the N $2p$, O $2s$, and O $2p$ states mixed together into the bonding MO's $2e'(\sigma)$ and $1a_2''(\pi)$ of the NO_3^- group. Band d represents MO $2a_1'(\sigma)$ composed mainly of the N $2s$, O $2s$, and O $2p$ atomic orbitals. Finally, features e and f reflect transitions from the strongly bonding MO's $1e'(\sigma)$ and $1a_1'(\sigma)$, with the essentially N $2p$-O $2s$ and N $2s$-O $2s$ character, respectively. An admixture of the Na s and p states into all valence MO's is found to be quite small. Note that only two occupied MO's ($1e''$ and $1a_2''$) are of π character, i.e., the respective electron densities are localized out of the anion plane, while other six MO's are localized in plane.

C. Resonant Auger decay and evidence for nuclear dynamics

The radiationless deexcitation of the intermediate state created by promotion of a core electron into an unfilled localized state below or slightly above the ionization threshold can follow several different pathways, as discussed, for example in Ref. 33. The Auger process can happen with the promoted electron acting as a spectator during the decay with the resulting two-hole final state [spectator Auger (SA) decay]. The screening effect of the spectator electron in the initial and final states of the Auger process leads to a high kinetic energy shift of the SA spectrum in comparison with the normal Auger (NA) one. Usually the spectrum becomes not only shifted but also complicated due to the interaction of the spectator and outgoing electrons. Additional complications of the spectral shape can be caused by shake-up and shake-down processes of the spectator electron in course of the deexcitation. Alternatively to the SA decay the electron promoted into the empty localized state can itself take part in the deexcitation creating a one-hole final state [participator Auger, (PA) decay]. This final state cannot be distinguished from that of the direct photoemission. As a result, PA decay may be observed as a resonant enhancement of intensity of individual spectral features and is sometimes called ''true resonant photoemission.'' It lies in the nature of the PA features that their kinetic energy shows linear dispersion (at least for free atoms) as a function of the photon energy, as is characteristic for the direct photoemission peaks. However, it is not trivial to observe this behavior (usually referred to as resonant Auger Raman effect), because of rather small natural width of the core-excited intermediate states. Only the use of narrow photon band excitation and high-resolution electron spectrometers has allowed demonstrating this effect.[34,35] Beside the SA and PA channels, NA decay can become an important pathway of deexcitation in solids and adsorbates if the time of hopping of the excited electrons to the neighboring sites does not exceed the resonance lifetime.

The decay of the nitrogen and oxygen core-excited intermediate states in $NaNO_3$ was investigated in this work by

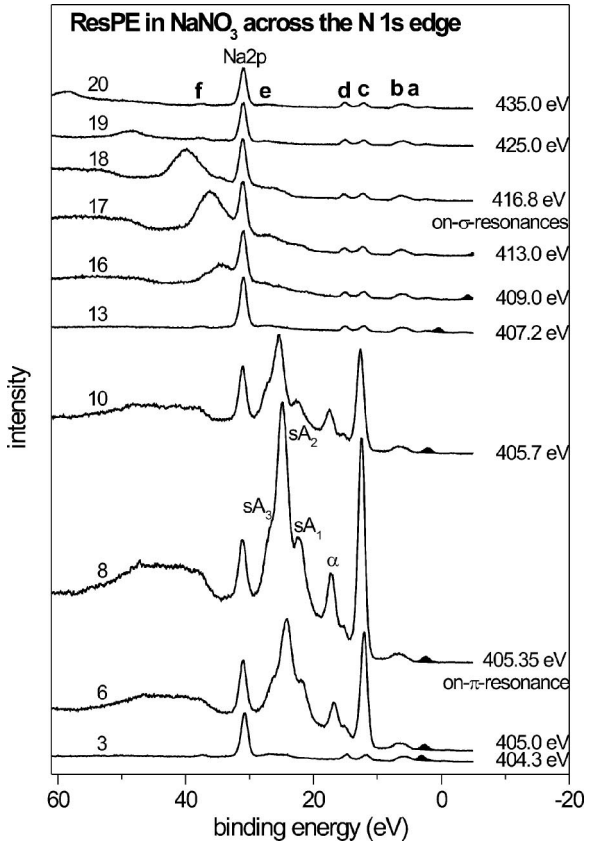

FIG. 3. Valence-band photoemission and Auger spectra of $NaNO_3$ taken with the excitation energy across the N 1*s* absorption edge. The second-order-light N 1*s* photolines are shadowed.

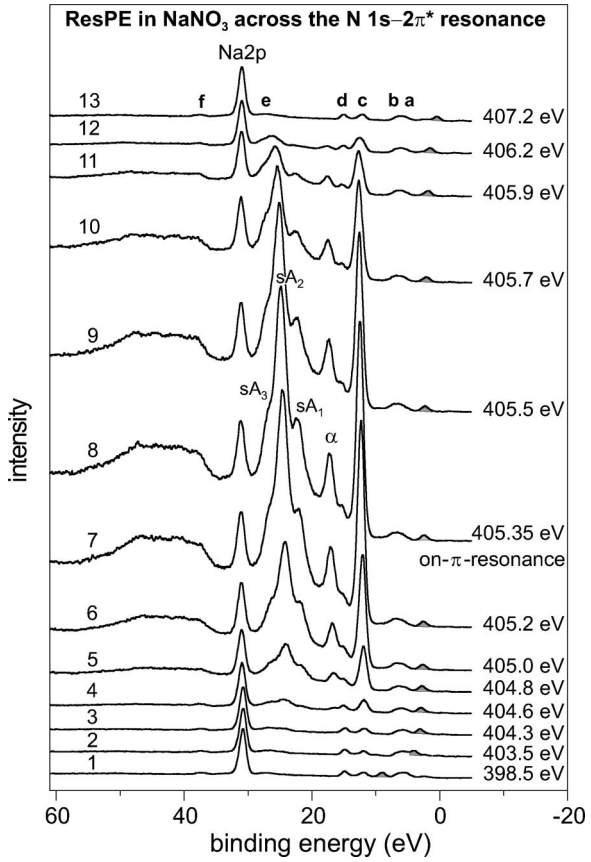

FIG. 4. Detailed view of the valence-band photoemission and Auger spectra of $NaNO_3$ taken with the excitation energy across the N $1s \rightarrow 2a_2''(\pi)$ resonance. The second-order-light N 1*s* photolines are shadowed.

means of resonant photoemission (Auger) spectroscopy with the photon energies covering the ranges 398–435 eV and 525–559 eV, respectively, as marked in the absorption spectra in Fig. 1. The resulting Auger spectra are shown in Figs. 3, 4 and 5, 6 for the photon excitations at the N 1*s* and O 1*s* absorption edges, respectively. We show two figures for each edge. The first ones (Figs. 3 and 5) provide an overview of the deexcitation spectra through the whole edges tracing the differences in decay of π and σ excitations. The other pair of figures (Figs. 4 and 6) represents the decay spectra at the most interesting regions of the N $1s^{-1}a_2''(\pi)$ and O $1s^{-1}a_2''(\pi)$ shape resonances, respectively. Spectral intensities are normalized to the incident photon flux. This normalization seems to be quite reasonable since it results in almost equal intensities of the Na $2p$ photoline, which indeed should remain almost constant due to the essentially anionic character of the lowest unoccupied π band and only minor changes in the Na $2p$ photoionization cross section in the respective spectral intervals. Small peaks originating from the second-order-light N 1*s* and O 1*s* core-level signals are shadowed. Their intensities remain constant too confirming once more the reliability of intensity normalization. The positions of the second-order-light photolines will be used for the exact calibration of the excitation energies in the further discussion of the dispersion behavior of individual features in the spectra. The spectra are plotted on the binding energy scale referring to the Fermi level of the spectrometer.

It can be clearly seen from Figs. 3 and 5 that the excitations into strongly localized π states ($1s \rightarrow 2a_2''$) and those into rather delocalized σ states ($1s \rightarrow 3a_1'$ and $1s \rightarrow 4e'$) decay very differently. Whereas a strong PA enhancement of the valence-band photolines, and a narrowing and structuring of the SA signals are characteristic in the region of the π-resonance, this behavior is not observed upon deexcitation of the σ resonances. This result resembles our findings for $NaNO_2$[5] and reveals again the importance of the intermediate-state localization. [We use here and thereafter the term ''photoline'' in order to underline the essentially molecular character of the valence-band photoemission in solid $NaNO_3$; however, the term ''band'' is also used throughout the text.]

First we will focus our attention on the decay spectra following the N $1s^{-1}a_2''(\pi)$ excitation (Fig. 4) numbered correspondingly to the photon energies used (marked in Fig. 1). The off-resonance spectra (1)–(3) at 398.5–404.3 eV and (13) at 407.2 eV demonstrate valence-band features $a-f$ and Na $2p$, which were already described in the previous section. With the photon energy scanning across the N $1s^{-1}a_2''(\pi)$ absorption peak from the off-resonance value of 404.3 eV to the on-resonance value of 405.35 eV the shape of the photoemission spectra changes dramatically. The reason for this change is the huge Auger electron emission due to both spectator and participator decay. The most prominent are the

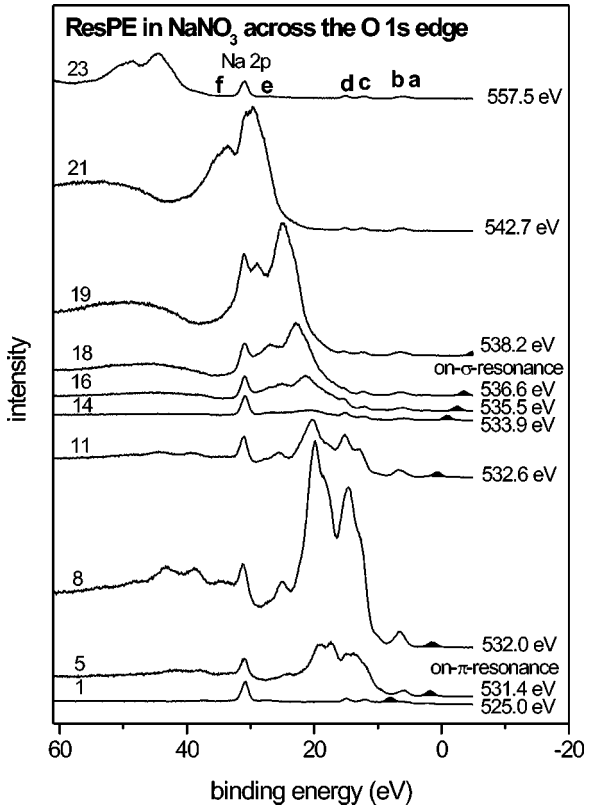

FIG. 5. Valence-band photoemission and Auger spectra of $NaNO_3$ taken with the excitation energy across the O 1*s* absorption edge. The second-order-light O 1*s* photolines are shadowed.

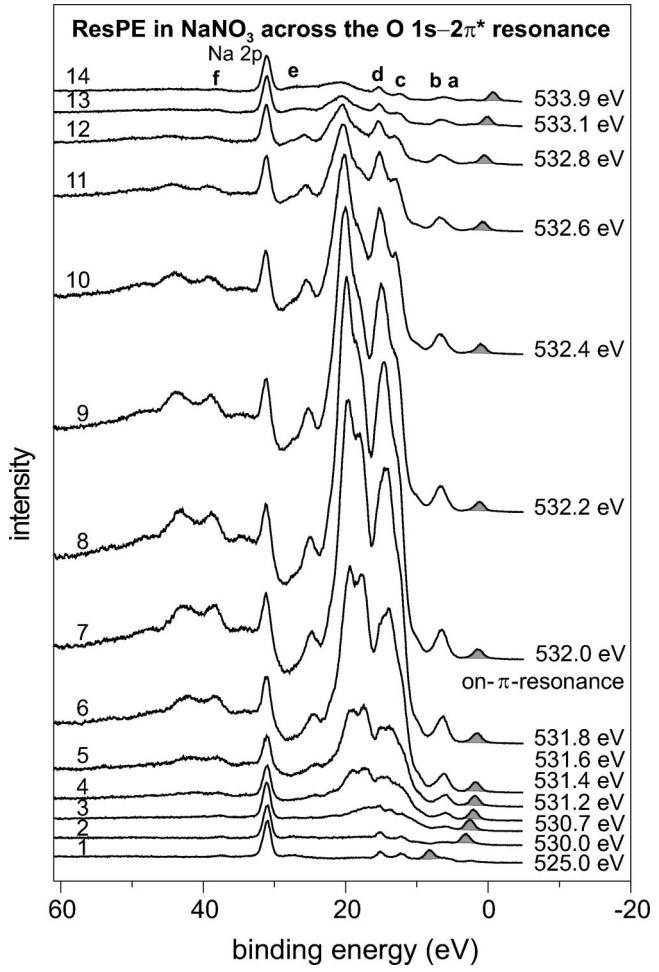

FIG. 6. Detailed view of the valence-band photoemission and Auger spectra of $NaNO_3$ taken with the excitation energy across the O $1s \rightarrow 2a_2''(\pi)$ resonance. The second-order-light O 1*s* photolines are shadowed.

$2p^{-2}$ SA features between 20 and 30 eV and the PA features between 4 and 16 eV binding energy. The broad $2p^{-1}2s^{-1}$ SA structures at 35-55 eV are also very strong in vicinity of the π resonance. Additionally, a highly intensive structure denoted α appears in the range between 16 and 20 eV, which can be definitely assigned neither to SA nor to PA, as will be discussed later.

The above assignment of the SA and PA energy regions correlates well with that made for the free BF_3 molecule.[9,13,14] Also the three-peak spectator structure sA_1-sA_2-sA_3 with energy separation of $\sim$4 eV between sA_1 and sA_3 (Fig. 4) resembles the corresponding SA structure in BF_3 at the B $1s^{-1}a_2''(\pi)$ resonance reported by Ueda *et al.*[9] and Simon *et al.*[13] indicating its similar origin in the BF_3 molecule and $NaNO_3$ crystal. A general similarity between the spectra of BF_3 at B $1s^{-1}a_2''(\pi)$ and those of $NaNO_3$ at N $1s^{-1}a_2''(\pi)$ can be observed also in the PA decay region, although the direct comparison would be not quite correct due to slightly different energy positions of the corresponding MO's in these two cases.

In the BF_3 spectra[9] the intensity of the group of overlapping $3e', 1e''$, and $1a_2'$ photolines, which is an analog of band *a*-*b* in the $NaNO_3$ valence-band spectra, is slightly increased (by a factor of 1.5) at the B $1s^{-1}a_2''(\pi)$ resonance. In turn, the intensity enhancement of spectral features caused by the partly resolved $2a_1', 2e'$, and $1a_2''$ MO's, which are analogical to *c*-*d* signals in Fig. 4, is of factor 4. In case of $NaNO_3$ at the N $1s^{-1}a_2''(\pi)$ resonance (Fig. 4) *a*-*b* structure is also only slightly enhanced by a factor of 1.5, while the situation with structures *c*-*d* differs from that in BF_3: signal *c* ($2e'$ and $1a_2''$) is dramatically amplified by a factor of 40, whereas signal *d* ($2a_1'$) is probably not amplified at all. Although the spectra of BF_3 were measured with lower resolution in comparison with those of $NaNO_3$, such a strong difference in intensity enhancement can hardly be explained by nonequivalent experimental conditions. Since the filled $1a_2''$ MO and the lowest unfilled $2a_2''$ MO have the same π symmetry, similar out-of-plane localization, and both are composed almost solely of N 2*p* and O 2*p* states, we suppose that it is the $1a_2''$ signal, which contributes most strongly into the huge enhancement of photoline *c* in Fig. 4. The larger number of 2*p* electrons in atomic nitrogen ($1s^2 2s^2 2p^3$ configuration) as compared to boron ($1s^2 2s^2 2p^1$) and the reduced 2*p* charge transfer from the central atom in NO_3^- as compared to BF_3 result in strongly increased probability of the most favorable autoionization decay channel with participation of two 2*p* electrons for core excitations localized on the central atom in $NaNO_3$. This fact provides the most-

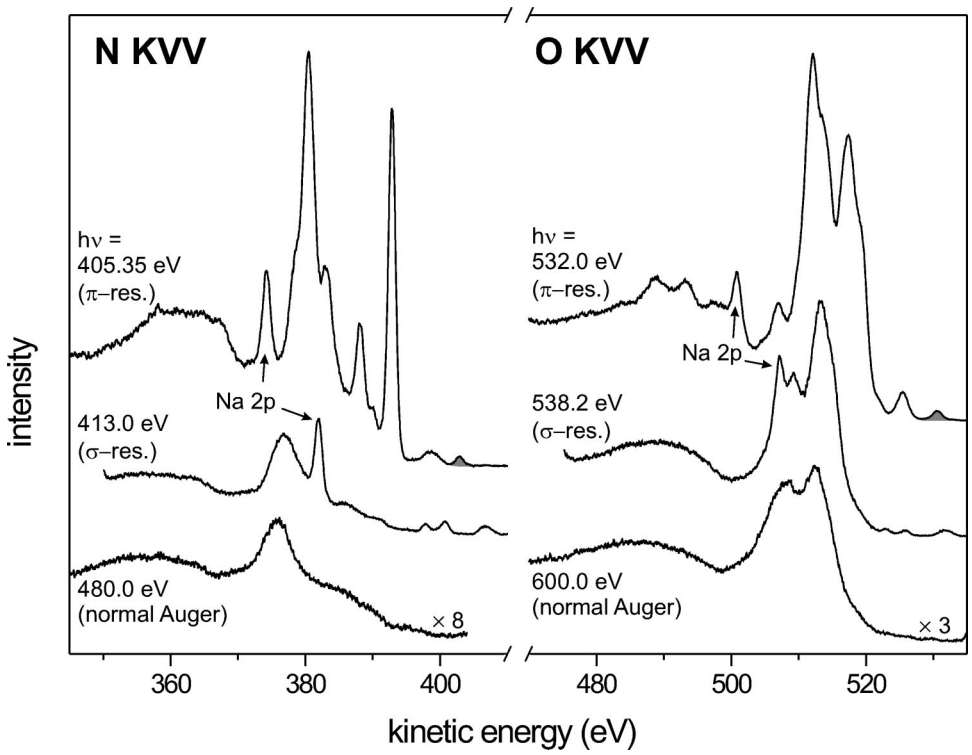

FIG. 7. Normal and excited at N(O) $1s\rightarrow\pi$ and $1s\rightarrow\sigma$ resonances N(O) *KVV* Auger spectra of solid $NaNO_3$ aligned with each other using kinetic energy scale. Excitation energies are indicated in the figure.

straightforward explanation for the 10 times stronger enhancement of feature *c* in this case, because it is a feature with a significant $2p$ contribution from the central atom (see Fig. 2). It should be noted that the evolution of the band *c* intensity upon crossing the N $1s^{-1}a_2''(\pi)$ resonance strictly follows the change in absorption, without any indications of the Fano-like profile shape. The reason for that is the strong domination of one channel of the ''true resonant photoemission'' (PA decay) over another channel (direct photoemission) resulting in only small interference effects.

A drastic increase in relative intensity in going from BF_3 to NO_3^- in $NaNO_3$ can be seen not only for the individual PA features but also for the SA decay. Indeed, in the BF_3 deexcitation spectra[9] the on-resonance SA intensity is not much larger than the off-resonance intensity of the photolines in the valence band. This is in evident contrast to the $NaNO_3$ decay spectra at the N $1s^{-1}a_2''(\pi)$ (Fig. 4) and O $1s^{-1}a_2''(\pi)$ (Fig. 6) resonances, where the SA intensity exceeds that of the off-resonance valence photolines *a*-*d* by factors of 40 and 50, respectively. The reasons for the difference in intensity of the SA signal between BF_3 and $NaNO_3$ are the same as those mentioned above for the PA signal.

In case of the Auger decay at the O $1s^{-1}a_2''(\pi)$ absorption peak (Fig. 6) it is more difficult to separate SA and PA features because of their partial overlap. Only the increase of the *a*-*b* band intensity (by a factor of 7 at the on-resonance excitation of 532.0 eV) can be definitely assigned to the PA channel. Among three MO's contributing into this band only the $1e''$ MO is of π character, being hence a candidate for highest amplification. The shape of the SA structures for both N $1s^{-1}a_2''(\pi)$ and O $1s^{-1}a_2''(\pi)$ excitations is rather complicated, being defined by many multiplet contributions. Therefore, it cannot be analyzed satisfactorily here, particularly in the case of the possible superposition of SA and PA channels. Note also that the shape of the SA signals changes upon scanning the excitation energy across both N and O $1s\rightarrow 2a_2''$ resonances. Further theoretical efforts are required for proper explanation of the SA signal's narrowing and varying of their spectral shape.

The importance of strong localization of the intermediate state for observing resonant features in decay spectra becomes evident in Fig. 7, which compares Auger spectra taken at the positions of *A* and *B* resonances in the absorption curve in Fig. 1 and the normal (far away off-resonance) Auger spectra on the common kinetic energy scale. In the case of excitation at the absorption band *A* the core electron is promoted into a highly localized π state, upon excitation at *B*—into a more delocalized (and probably hybridized with Na $3s$) σ state, and in case of NA into a completely delocalized continuum state of plane-wave-like character. It is evident that only in case of π excitation both SA and PA resonant features can be clearly seen in the spectra. Some SA nature of the decay resulting from the σ excitation can still be noticed due to a 1 eV shift of the main Auger structures to higher kinetic energies in respect with the NA structures, as well as in their slightly different shape. However, these remains of resonant behavior are rather insignificant in comparison with the case of π deexcitation.

It has been mentioned in the above discussion of asymmetrical shape of the N and O $1s\rightarrow 2a_2''$ absorption peaks that the processes of electronic decay and vibrational motion inside the NO_3^- group lie on the same time scale. Before we consider whether and how nuclear dynamics manifests itself in the decay spectra of $NaNO_3$, the same dynamical aspect in case of electronic decay of the B $1s\rightarrow 2a_2''$ core excitation in a gas-phase BF_3 molecule will be shortly addressed by sum-

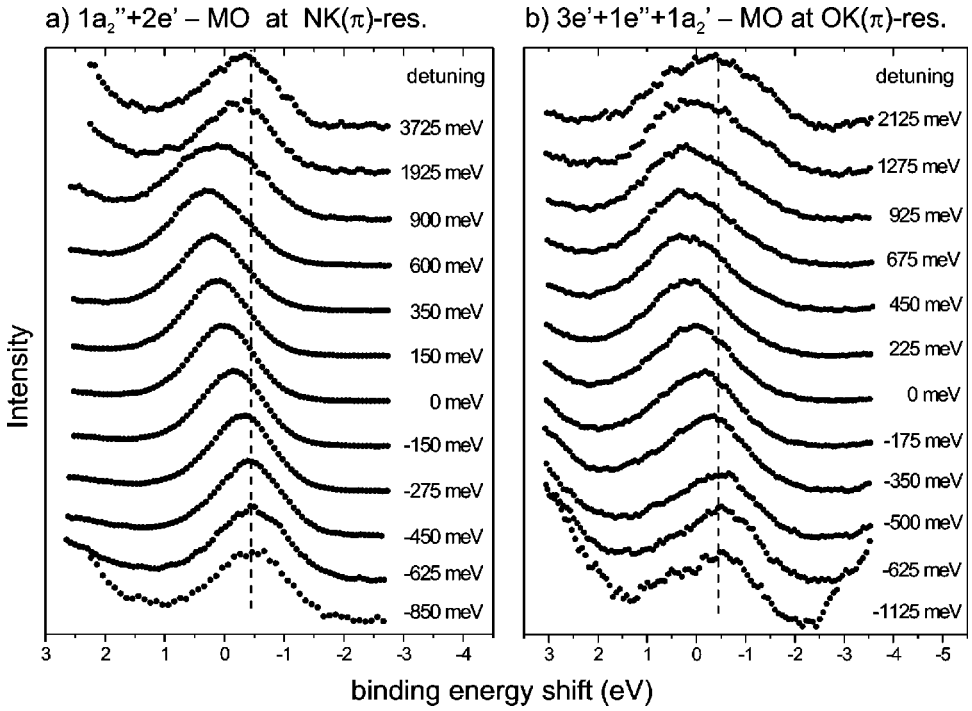

FIG. 8. Evolution of the shape and energy positions of some valence-band photolines as a function of excitation detuning from the position of the corresponding π resonance: (a) $1a_2''+2e'$ MO at N $1s^{-1}\pi$ (feature *c* in Fig. 4); (b) $3e'+1e''+1a_2'$, MO at O $1s^{-1}\pi$ (feature *a*-*b* in Fig. 6). The data are normalized to the same peak intensity.

marizing the results of Ueda *et al.*,[9] Simon *et al.*,[13] and Tanaka *et al.*[14] The binding energies of the PA peaks were found to be constant; i.e., the respective kinetic energies demonstrate strictly linear dependence on the photon energy. In contrast, the kinetic energies of the SA features were found to be nearly constant. These facts were interpreted in terms of a difference in the shape of the adiabatic potential surfaces along the axis of out-of-plane atomic displacements (a_2'' vibration) for the SA and PA final states. The evolution of the wave packet along the potential surfaces of the intermediate a_2'' state and final PA state accompanying the out-of-plane movement of the boron atom has been directly observed in the decay spectra as PA satellite structures (a tail) shifted by 2.25 eV to lower kinetic energies (the so-called dynamical Auger emission). Thus, these satellites were associated with the participator decay taking place in the C_{3v} geometry of BF_3. The longer is the lifetime of the B $1s^{-1}2a_2''$ intermediate state, the stronger are these satellites.[14]

Let us now consider the situation with the energy positions of individual PA peaks upon the decay of the N $1s \rightarrow 2a_2''$ and O $1s \rightarrow 2a_2''$ shape resonances in solid $NaNO_3$. The most appropriate candidates for such an analysis are the strongly resonating valence-band structure *c* in case of the N $1s \rightarrow 2a_2''$ absorption and the weaker resonating structure *a*-*b* in case of the O $1s \rightarrow 2a_2''$ absorption. In Fig. 8 the evolution of both these bands upon crossing the above-mentioned absorption resonances is presented. All spectra are normalized to equal peak intensity in order to facilitate the examination of their shape and energy positions. The photon energies of detuning from the on-resonance position are not simply the monochromator readings. They were additionally calibrated using the position of the second-order-light N 1*s* and O 1*s* photolines. The Raman-like behavior typical for the PA in atomic systems and reported also in case of BF_3 is indicated by dashed vertical lines as a guidance for the eye. Even without any quantitative analysis a significant deviation of the energy positions of both *c* and *a*-*b* bands upon scanning across the N $1s \rightarrow 2a_2''$ and O $1s \rightarrow 2a_2''$ resonances, respectively, is evident from Fig. 8. However, it is more meaningful to analyze the positions of center of gravity (CG) for each spectral feature instead of the maximum intensity positions, because of the obvious asymmetry in some spectra. We have consequently subtracted a smooth monotonous background and then have computed the CG positions for each peak in Fig. 8. The result of this procedure is shown in Fig. 9, where the kinetic energy shift of the CG positions is presented as a function of the photon energy detuning from the corresponding resonance. Evidently, the non-Raman behavior can be documented also for the CG of both participator lines in the π-resonance region.

Several possible reasons for the observed deviations should be analyzed. First, one could argue that both *c* and *a*-*b* features represent envelopes of two and three different MO's, respectively, which could be nonequivalently enhanced upon crossing the resonances, resulting in a changing asymmetry of the envelopes. This explanation can be definitely ruled out. Indeed, in this case the experimental points in Fig. 9 would run parallel to the Raman-law line in close vicinity to the on-resonance point, because the changes in asymmetry of the envelopes are minor if the intensity of one individual MO in the envelope is much larger than the intensities of others. Contrary to this expectation, the experimental points experience the strongest deviation from the Raman law exactly in the close vicinity to the resonance. There is a risk of another artificial effect possibly contributing into the deviations from the Raman-like dispersion. It can result from the convolution of the photon band shape with the shape of

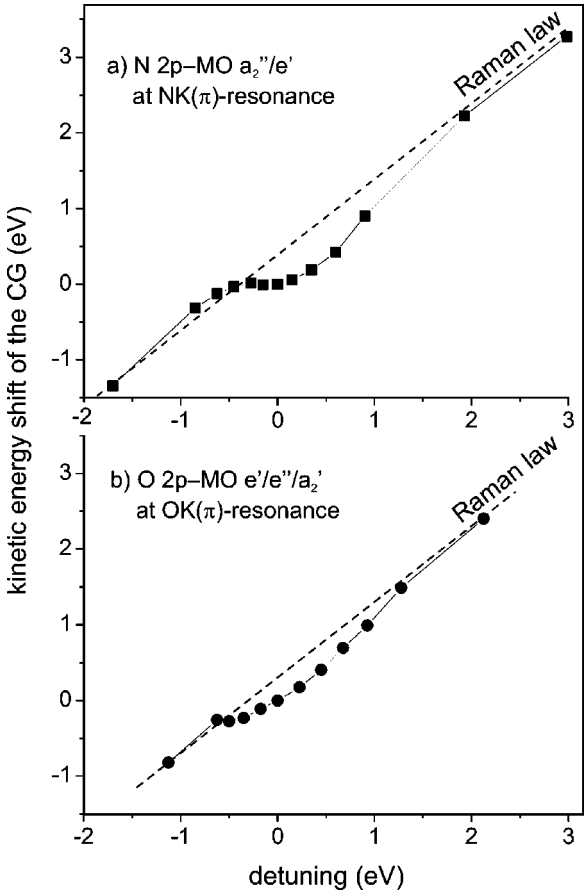

FIG. 9. Kinetic energy shift of the CG (center of gravity) positions of the peaks shown in Fig. 8 as a function of excitation detuning from the corresponding resonance positions. Dashed lines indicate linear-dispersion behavior (Raman law).

lifetime broadening of core-excited states as predicted by Gel'mukhanov and Ågren[36] and observed by Kukk *et al.*[37] However, also this effect can hardly explain the observed behavior of the CG positions, because the deviations about the line of linear dispersion are highly asymmetric below and above the point of resonance. Moreover, this apparatus effect should be stronger for the broadband excitation,[38] which is not the case in our experiment.

As the most probable explanation of the observed nonlinear dispersion in the PA decay we propose a partial conversion of the electron kinetic energy into vibrational motion of the NO_3^- anion. Gel'mukhanov and Ågren[38] have shown that such non-Raman (and even anti-Raman) behavior of the CG of resonantly scattered electrons can be explained for molecular systems in terms of interplay between the parameters defining the potential surfaces of the involved intermediate and final states. The difference in behavior of the PA features between the cases of $NaNO_3$ and BF_3 may be assigned to the fact that the fast dissociation, which is possible in the BF_3 molecule, probably becomes suppressed for the NO_3^- anion surrounded by six Na^+, thus providing more time for vibrational motion in the excited state. There is one more consideration justifying this assignment. Namely, if the NO_3^- anion has more time for vibrational motion in the core-excited intermediate state than the free BF_3 molecule, the low-kinetic-energy satellite structure observed in the PA decay of BF_3 (Ref. 9) and interpreted as a signature of dynamical Auger emission[13,14] should become more pronounced in case of $NaNO_3$. In the above discussion of decay spectra in Fig. 4 we have mentioned that a strong peak α could be definitely assigned neither to SA nor to PA features. Peaks α and c change their energy positions and intensities almost synchronously upon crossing the N $1s\rightarrow 2a_2''$ resonance (energy separation 4.65 eV), so that α may be interpreted as a low-kinetic-energy satellite of c resulting from dynamical Auger emission in the C_{3v} geometry of NO_3^-. If this interpretation is correct, the higher intensity of peak α in comparison with the respective satellite structures in case of BF_3 is a direct consequence of the partly suppressed fragmentation in $NaNO_3$.

IV. CONCLUSIONS

By example of $NaNO_3$ we have shown that ionic-molecular crystals are very interesting and promising objects for synchrotron radiation research. Not only their electronic structure but also the nuclear motion accompanying the decay processes of their core excitations can be successfully studied by means of x-ray absorption and resonant Auger spectroscopy. This becomes possible due to the unique combination of molecular and solid-state properties in these crystals resulting from the quasi-isolated location of their polyatomic anions.

It has been demonstrated that the most prominent features in the electronic structure of both valence and conduction bands in $NaNO_3$ are determined by MO's of the NO_3^- group. In particular, pronounced resonances *A*, *B*, and *C* in the N 1*s* and O 1*s* absorption spectra are assigned on the basis of comparison with the B 1*s* absorption and *e*-BF_3 scattering spectra of the BF_3 molecule, which is isoelectronic and isostructural to NO_3^-, to the transitions into the conduction-band states associated with MO's $2a_2''(\pi), 3a_1'(\sigma)$ and $4e'(\sigma)$ of the NO_3^- anion, respectively. The rather unusual structure of the conduction band with a low-lying narrow subband *A* separated from the subsequent broadbands *B*-*C* by a gap of several eV is caused by a strong anisotropy of the molecular potential of the NO_3^- group, resulting in a strong energy separation between $\pi(2p_z)$ and $\sigma(2p_{x,y})$ MO's.

Strong resonant effects have been observed in the Auger decay following the N $1s\rightarrow 2a_2''(\pi)$ and O $1s\rightarrow 2a_2''(\pi)$ core excitations. Both spectator and participator decay channels can be clearly seen in the deexcitation spectra. The amplification coefficients caused by PA decay are very high. The most pronounced enhancement by a factor of 40 is characteristic for the photoline associated with the group of $1a_2''$ and $2e'$ MO's of the NO_3^- anion at the N $1s\rightarrow 2a_2''(\pi)$ resonance (peak *c* in Fig. 4). The on-resonance SA signals for both nitrogen and oxygen deexcitation spectra are considerably shifted, narrowed, and structured in comparison with the corresponding NA signals, and their intensities exceed those of the PA decay. In turn, only minor resonant effects (with a domination of the SA decay) have been found in the

Auger spectra following the less localized N (O) $1s \rightarrow \sigma$ ($3a_1'$ and $4e'$) excitations. All these findings resemble the results for the gas-phase BF_3 molecule, thus providing strong evidence for the quasi molecular nature of nitrogen and oxygen core excitations in solid $NaNO_3$.

A reflection of vibrational properties of the NO_3^- anion has been observed both in the N 1*s* and O 1*s* absorption spectra and in the Auger spectra following N and O π excitations. In the N 1*s* and O 1*s* absorption curves the out-of-plane vibration in NO_3^- manifests itself in the asymmetrical shape of the corresponding π resonances resulting from the unresolved progression of the a_2'' vibrational levels. In the electronic decay spectra of the N and O π excitations nuclear motion inside the NO_3^- anion is reflected in the strongly non-Raman dispersion of the CG of some valence photolines upon scanning the photon energy across the corresponding resonances. In spirit of Gel'mukhanov and Ågren[38] we assign this behavior to a partial conversion of electron kinetic energy into the vibrational motion of NO_3^- as a consequence of the interplay between the parameters defining the potential surfaces of the involved intermediate and final states. Additionally, peak α in Fig. 4 may represent the effect of dynamical Auger emission observed previously only in free molecules. To our knowledge these results represent the first experimental observation of nuclear dynamics in a solid made by means of resonant Auger spectroscopy.

ACKNOWLEDGMENTS

We wish to thank S. Gorovikov and M. Leandersson for valuable technical assistance in MAX-lab and A. A. Pavlychev for stimulating discussions. A.S.V. gratefully acknowledges the financial support of Institut für Oberflächen- und Mikrostrukturphysik der Technischen Universität Dresden and W.-Ostwald-Institut für Physikalische und Theoretische Chemie der Universität Leipzig. This work was supported by Russian Foundation for Basic Research, Grant No. 01-03-32285, and by the Deutsche Forschungsgemeinschaft, Grant No. FOR 404 and SFB 463, TPB4.

*Present address: MAX-lab, Lund University, S-22100 Lund, Sweden.

[1] J.W. Allen, in *Synchrotron Radiation Research—Advances in Surface and Interface Science*, edited by R. Z. Bachrach (Plenum New York, 1992), Vol. 1 p. 253.
[2] J. Stöhr, *NEXAFS Spectroscopy*, Springer Series in Surface Science, Vol. 25 (Springer, Berlin, 1992).
[3] W. Eberhardt, in *Application of Synchrotron Radiation*, Springer Series in Surface Science, Vol. 35, edited by W. Eberhardt (Springer, Berlin, 1995), p. 203.
[4] N. Mårtensson, O. Karis, and A. Nilsson, J. Electron Spectrosc. Relat. Phenom. **100**, 379 (1999).
[5] A.S. Vinogradov, A.B. Preobrajenski, S.L. Molodtsov, S.A. Krasnikov, R. Szargan, A. Knop-Gericke, and M. Hävecker, Chem. Phys. **249**, 249 (1999).
[6] A.F. Wells, *Structural Inorganic Chemistry* (Clarendon Press, Oxford, 1984).
[7] S.V. Nekipelov, V.N. Akimov, and A.S. Vinogradov, Fiz. Tverd. Tela (Leningrad) **30**, 3647 (1988) [Sov. Phys. Solid State **30**, 2095 (1988)].
[8] A.A. Pavlychev, A.S. Vinogradov, V.N. Akimov, and S.V. Nekipelov, Phys. Scr. **41**, 160 (1990).
[9] K. Ueda, H. Chiba, Y. Sato, T. Hayaishi, E. Shigemasa, and A. Yagishita, J. Chem. Phys. **101**, 3520 (1994).
[10] K. Ueda, K. Ohmori, M. Okunishi, H. Chiba, Y. Shimizu, Y. Sato, T. Hayaishi, E. Shigemasa, and A. Yagishita, Phys. Rev. A **52**, R1815 (1995).
[11] M. Simon, P. Morin, P. Lablanquie, M. Lavollée, K. Ueda, and N. Kosugi, Chem. Phys. Lett. **238**, 42 (1995).
[12] K. Ueda, in *Atomic and Molecular Photoionization*, Proceedings of the Oji International Seminar, edited by A. Yagishita and T. Sasaki (Universal Academy, Tokyo, 1996), p. 139.
[13] M. Simon, C. Miron, N. Leclercq, P. Morin, K. Ueda, Y. Sato, S. Tanaka, and Y. Kayanuma, Phys. Rev. Lett. **79**, 3857 (1997).
[14] S. Tanaka, Y. Kayanuma, and K. Ueda, Phys. Rev. A **57**, 3437 (1998).
[15] E. Ishiguro, S. Iwata, Y. Suzuki, A. Mikuni, and T. Sasaki, J. Phys. B **15**, 1841 (1982).
[16] M. Tronc, L. Malegat, R. Azria, and Y. Le Coat, J. Phys. B **15**, L253 (1982).
[17] A.S. Vinogradov and V.N. Akimov, Phys. Low-Dimens. Semicond. Struct. **4/5**, 63 (1994).
[18] S. Göttlicher and C.D. Knöchel, Z. Kristallogr. **148**, 101 (1978).
[19] H. Yamashita and R. Kato, J. Phys. Soc. Jpn. **29**, 1557 (1970).
[20] M.I. McCarthy, K.A. Peterson, and W.P. Hess, J. Phys. Chem. **100**, 6708 (1996).
[21] K. Nakamoto, *Infrared and Raman Spectra of Inorganic and Coordination Compounds* (Wiley, New York, 1997) Pt. A, Sec. II.
[22] K.C. Prince, M. Vondráček, J. Karvonen, M. Coreno, R. Camilloni, L. Avaldi, and M. de Simone, J. Electron Spectrosc. Relat. Phenom. **101-103**, 141 (1999).
[23] J.F. Wyatt, I.H. Hillier, V.R. Saunders, J.A. Connor, and M. Barber, J. Chem. Phys. **54**, 5311 (1971).
[24] S.P. Dolin and M.E. Dyatkina, J. Struct. Chem. **13**, 906 (1972).
[25] L.E. Harris, J. Chem. Phys. **58**, 5615 (1973).
[26] M.C. Payne, M.P. Teter, D.C. Allan, T.A. Arias, and J.D. Joannopoulos, Rev. Mod. Phys. **64**, 1045 (1992).
[27] W. Kohn, Rev. Mod. Phys. **71**, 1253 (1999).
[28] Molecular Simulations Inc., *CASTEP User's Guide*, San Diego (2000).
[29] J.P. Perdew and A. Zunger, Phys. Rev. B **23**, 5048 (1981).
[30] J.P. Perdew and Y. Wang, Phys. Rev. B **45**, 13 244 (1992).
[31] D. Vanderbilt, Phys. Rev. B **41**, 7892 (1990).
[32] H.J. Monkhorst and J.D. Pack, Phys. Rev. B **13**, 5188 (1976).
[33] H. Aksela and S. Aksela, J. Electron Spectrosc. Relat. Phenom. **100**, 395 (1999).
[34] A. Kivimäki, A. Naves de Brito, S. Aksela, H. Aksela, O.-P. Sairanen, A. Ausmees, S.J. Osborne, L.B. Dantas, and S. Svensson, Phys. Rev. Lett. **71**, 4307 (1993).
[35] Z.F. Liu, G.M. Bancroft, K.H. Tan, and M. Schachter, Phys. Rev. Lett. **72**, 621 (1994).
[36] F. Gel'mukhanov and H. Ågren, Phys. Rev. A **49**, 4378 (1994).
[37] E. Kukk, S. Aksela, and H. Aksela, Phys. Rev. A **53**, 3271 (1996).
[38] F. Gel'mukhanov and H. Ågren, Phys. Rev. A **54**, 3960 (1996).